Calcolo manuscript No.
(will be inserted by the editor)

Fourier Analysis of Diamond Discretization in Particle Transport

Guillaume Bal

Department of Mathematics, University of Chicago, Chicago, IL 60637, USA
gbal@math.uchicago.edu

The date of receipt and acceptance will be inserted by the editor

Abstract. This paper theoretically and numerically analyzes the Diamond Discretization (DD) of free particle transport equations. DD is one of the most commonly used discretizations used in particle transport theory, with applications ranging from the propagation of neutrons in nuclear physics to that of near infra red photons in medical imaging. Based on the theory of scalar hyperbolic equations in the Fourier domain, we show that DD performs very well when the boundary data are smooth and the absorption coefficient small. However, because high frequency modes are not damped at all by DD even in the dissipative case, several unphysical modes appear when the boundary conditions are not so smooth. These spurious oscillations are analyzed carefully and displayed numerically.

1. Introduction

Linear transport equations are used to model the propagation of particles and that of the energy density of high frequency waves in scattering media. The particle description arises in physical phenomena such as neutrons in nuclear reactor physics and electrons and photons in radiotherapy [3,6,9,13]. The wave description, leading to the theory of radiative transfer, models the propagation of electromagnetic waves in turbulent atmosphere and that of earthquake generated shear waves in the earth's crust [5,7,14,20,21].

These novel applications along with the fast growing performances of modern computers have triggered the development of new computer codes to solve the transport equations, for instance in medical imaging, where non-destructive near-infra-red (NIR) photons are increasingly being used to monitor certain properties of human tissues [3,4,13].

One of the most popular transport discretizations is based on the discrete ordinates method to discretize the velocity domain and the Diamond Discretization (DD) to discretize the spatial variables. We refer to [9,17] for the details of the method. The reason for its popularity is that DD is second-order accurate and relatively straightforward to implement numerically. The main result of interest in this paper is that DD can be seen as a finite difference method used to discretize linear dissipative first-order scalar hyperbolic equations, which are obtained from the velocity discretization of the full transport equations. The analysis of finite difference discretization of such equations, at least in the conservative case, has been addressed for quite a long time in the literature. We refer for instance to [2,11,12,15,19,22] and references therein. The analysis in these references is based on working in the Fourier domain. Many spurious modes are generated when particles travel across a uniform mesh and the Fourier analysis is the right tool to analyze the behavior of these modes.

Unlike the general theories in the references mentioned above, where general classes of finite difference methods are theoretically analyzed, we restrict ourselves in this paper to the analysis of Diamond Discretization. Unlike many classical second-order discretizations such as the Lax-Wendroff scheme, DD turns out to be an L^2-isometry in the conservative case, a distinguished property implying that high frequencies, which cannot be accurately resolved by any finite difference method, are not damped out by the numerical scheme. An immediate consequence is that irregular boundary conditions yield poor resolution and heavy spatial oscillations. Such a fact has recently been evidenced numerically by Mathews [18]. Nonetheless, as irregular as DD may be, smooth moments of the discretized solution showed very good convergence properties. This observation was for instance put forward numerically in [16]. This paper theoretically analyzes the oscillations that can occur in the Diamond Discretization of boundary value problems and provides a satisfactory understanding of the numerical observations in [16,18]. Several numerical simulations that underline the theoretical results are also presented.

The paper is organized as follows. Section 2 is devoted to a presentation of the linear transport equation, its Diamond Discretization and its formulation in the Fourier domain. The following three sections analyze the outgoing solution of the boundary value transport problem discretized by using DD. Section 3 deals with the L^2-theory of DD in the conservative case. Section 4 addresses the analysis of local error estimates for boundary conditions of the form of delta or Heaviside functions. The whole range of oscillations generated by DD is carefully displayed. Section 5 is devoted to the dissipative case. Next, section 6 considers the estimate of two-dimensional moments of the discretized solution and shows an improved convergence rate over that of the outgoing solution. Finally, we present in section 7 some numerical simulations that show that the theoretical estimates of the previous sections are optimal.

2. Fourier Analysis of Diamond Discretization

The linear first-order hyperbolic transport equation we consider in this paper is given by

$$\begin{aligned} &\beta \cdot \nabla u + \gamma u = 0 \qquad \text{in} \quad \Omega, \\ &u = g \qquad \text{on} \quad \Gamma_0, \end{aligned} \tag{1}$$

where $\Omega = (0, L) \times (0, 1)$ in $I\!R^2$, with $L > 0$, $\beta = (\mu, \nu)$ is a normalized constant vector, γ is a constant non negative absorption term and

$$\Gamma_k = \partial\Omega \cap \{(x, y) \in I\!R^2 \text{ s.t. } y = k\}, \qquad k = 0, 1. \tag{2}$$

The source term g is given. We are interested in the diamond discretization (DD) of the solution u to (1). In the following three sections, we focus on the outgoing distribution $u_{|\Gamma_1}$. Section 6 then considers twodimensional errors of the solutions and its moments in the whole domain Ω.

To discretize (1), we use the Diamond Discretization on a uniform rectangular grid composed of $LN \times N$ identical squares of area $h \times h$ where $h = N^{-1}$. We denote the flux on the edges of the discretization by

$$U_k^n \approx u((k - \frac{1}{2})h, nh) \quad \text{for} \quad 1 \le k \le LN \ \text{ and } 0 \le n \le N.$$

We denote by $U^n(x) = U_k^n$ for $x \in ((k-1)h, kh)$. The boundary condition is $U^0(x) = g(x)$, which is constant on each edge of the discretization in numerical simulations, and extended to 0 outside Γ_0.

The Diamond Discretization is constructed as follows

$$\begin{aligned} U_k^{n+1} &= \alpha_{HH} U_k^n + \alpha_{VH} V_{k-1}^{n+1} \\ V_k^{n+1} &= \alpha_{HV} U_k^n + \alpha_{VV} V_{k-1}^{n+1}, \end{aligned} \tag{3}$$

for $k \in Z$ and $0 \leq n \leq N$. The terms V_k^{n+1} correspond to the value of the flux on the vertical edges of the discretization. The coefficients in (3) are given by

$$\begin{aligned} \alpha_{HH} &= \frac{\nu - \mu - \gamma h/2}{\nu + \mu + \gamma h/2} & \alpha_{HV} &= \frac{2\nu}{\nu + \mu + \gamma h/2} \\ \alpha_{VH} &= \frac{2\mu}{\nu + \mu + \gamma h/2} & \alpha_{VV} &= \frac{\mu - \nu - \gamma h/2}{\nu + \mu + \gamma h/2}. \end{aligned} \tag{4}$$

These coefficients are obtained as follows. We assume that the discrete solution is constant on every edge of the discretization. The exact integration of the transport equation (1) over each cell gives one equation per cell. The second equation is obtained by assuming that the average of the fluxes on the upper and lower edges equals the average of the fluxes on the left and right edges. We refer to [17] for additional details.

Let us now eliminate the V_k^{n+1}'s in (3). By induction, we get

$$U_k^{n+1} = \sum_{m=1}^{\infty} \alpha_{HV}(\alpha_{VV})^{m-1}\alpha_{VH} U_{k-m}^n + \alpha_{HH} U_k^n. \tag{5}$$

Therefore, as functions of x, we have

$$U^{n+1}(x) = \sum_{m=1}^{\infty} \alpha_{HV}(\alpha_{VV})^{m-1}\alpha_{VH} U^n(x - mh) + \alpha_{HH} U^n(x). \tag{6}$$

Because of the boundary conditions, only a finite number of the terms in the above sum are non zero. We define the Fourier transform as

$$\hat{U}(\xi) = \int e^{ix\xi} U(x) dx. \tag{7}$$

Taking now the Fourier transform of (6) yields

$$\hat{U}^{n+1}(\xi) = \sum_{m=1}^{\infty} \alpha_{HV}(\alpha_{VV})^{m-1}\alpha_{VH} e^{imh\xi} \hat{U}^n(\xi) + \alpha_{HH} \hat{U}^n(\xi). \tag{8}$$

This is equivalent to

$$\hat{U}^{n+1}(\xi) = \Big[\alpha_{HH} + \frac{\alpha_{HV}\alpha_{VH} e^{ih\xi}}{1 - \alpha_{VV} e^{ih\xi}}\Big] \hat{U}^n(\xi) \equiv R(h\xi)\hat{U}^n(\xi). \tag{9}$$

We also obtain that $\hat{U}^n(\xi) = (R(h\xi))^n \hat{U}^0(\xi)$. Therefore, we have to understand the behavior of $R^n(h\xi)$ and compare it with $e^{inh\xi\mu/\nu} e^{-\gamma nh/\nu}$, which is the Fourier multiplier for the exact solution, since we can verify that $\hat{u}(\xi, nh) = e^{inh\xi\mu/\nu} e^{-\gamma nh/\nu} \hat{g}(\xi)$. Here, $\hat{u}(\xi, nh)$ stands for the Fourier transform of $u(x,nh)$ in the first variable only. Notice also that the exact solution satisfies $u(x,nh)=e^{-\gamma nh/\nu}g(x-nh\mu/\nu)$.

We consider here only the Diamond Discretization. However, most of our results hold for numerical schemes that have the Fourier representation $\hat{U}^n(\xi)=R^n(h\xi)\hat{U}^0(\xi)$, where the multiplier R can take a more general form than in (9).

The theory of finite differences is very extensive. we refer to [19,22] and references therein; see also the recent review in Part I in [8]. We now present a self-contained description of Diamond Discretization, even though some results, particularly in the L^2 analysis, have already been obtained in the literature. The results on the characterization of the spatial localization of oscillations in section 4, on the role of absorption in section 5 and on the moment estimates in sections 3 and 6 seem to be new.

3. L^2 analysis in the conservative case

We assume first that $\gamma=0$. This case retains most of the theoretical difficulties of the general problem and is considered first because its presentation is somewhat simpler. Since then $\alpha_{VV}=-\alpha_{HH}$ and denoting by $\alpha=\alpha_{HH}$ to simplify, we have

$$R(h\xi)=\frac{\alpha+e^{ih\xi}}{1+\alpha e^{ih\xi}}.$$

We recast R as

$$R(h\xi)=e^{i\theta(h\xi)}, \tag{10}$$

where

$$\theta(h\xi)=\arctan\Big(\frac{(1-\alpha^2)\sin(h\xi)}{2\alpha+(1+\alpha^2)\cos(h\xi)}\Big). \tag{11}$$

This shows that $|R(h\xi)|\equiv 1$. Therefore, no frequency is absorbed by the scheme, which will be well posed in L^2, but not in other L^p spaces [11,22]. Let us denote by $U_h(x)=U^N(x)$, that is to say the discrete solution on the outgoing edge of Ω. We now compare it to the exact solution $U(x)=u(x,1)$. For an incoming boundary condition g, both solutions are given by

$$U_h(x)=\frac{1}{2\pi}\int e^{-ix\xi}\, e^{\dfrac{i}{h}\theta(h\xi)}\;\hat{g}(\xi)d\xi \tag{12}$$

$$U(x)=\frac{1}{2\pi}\int e^{-ix\xi} e^{i\dfrac{\mu}{\nu}\xi}\;\hat{g}(\xi)d\xi. \tag{13}$$

We equip $L^2(\mathbb{R})$ with its usual norm $\|\cdot\|$ and denote by $\|\cdot\|_s$ the norm of the Sobolev space $H^s(\mathbb{R})$ [1]. For $s \in \mathbb{N}$, the space $H^s(\mathbb{R})$ is the space of functions with all derivatives up to order s in $L^2(\mathbb{R})$. An equivalent definition, which also holds for non integer values of $s \geq 0$ is

$$\begin{aligned} &H^s(\mathbb{R}) = \{f(x) \in L^2(\mathbb{R}) \text{ such that } \|f\|_s < \infty\}, \qquad \text{where} \\ &\|f\|_s = \Big(\int |\hat{f}(\xi)|^2 (1+|\xi|^2)^s d\xi \Big)^{1/2}. \end{aligned} \tag{14}$$

Here, $\hat{f}(\xi)$ denotes the Fourier transform of $f(x)$. Notice that $H^0(\mathbb{R}) = L^2(\mathbb{R})$.

Remark 1. The H^s norm with non integer values of s is also useful. For instance, recall that the step function $g(x) = 1$ on (a,b) and $g(0) = 0$ outside (a,b) is in $H^s(\mathbb{R})$ for all $s < 1/2$. The same regularity holds for every piecewise constant function with compact support. Also, a piecewise linear continuous function with compact support is in every $H^s(\mathbb{R})$ such that $s < 3/2$.

The main result of this section is as follows.

Theorem 1. *We assume that $\mu \neq \nu$ and $\nu > 0$. Let $g \in H^s(\mathbb{R})$. Then $U(x) \in L^2(\mathbb{R})$, $U_h(x) \in L^2(\mathbb{R})$, and*

$$\|U\| = \|U_h\| = \|g\|. \tag{15}$$

For all s, t, such that $0 \leq t \leq s \leq 3$, we have

$$\|U_h - U\|_t \leq C h^{\frac{2(s-t)}{3}} \|g\|_s = C h^{\frac{2(s-t)}{3}} \|U\|_s. \tag{16}$$

Moreover, let $g \in H^t(\mathbb{R})$ and $p \in H^s(\mathbb{R})$. Then the moments of the solution to the convection equation (1) satisfy the following estimate, for $s \geq 0$ and $t \geq 0$ such that $t + s \leq 3$,

$$\Big| \int p(x)(U_h(x) - U(x))dx \Big| \leq C h^{\frac{2(s+t)}{3}} \|g\|_t \, \|p\|_s. \tag{17}$$

Before proving this theorem, let us start with several remarks.

Remark 2. The theorem shows that the regularity of the outgoing flux for DD strongly depends on the regularity of the incoming distribution. However, for incoming distributions in $L^2(\mathbb{R})$, the moments of the error still display an error of order h^2 provided $g \in H^3(\mathbb{R})$. This result in agreement with the numerical simulations in [16]. It also displays one advantage of the analysis in the Fourier domain; namely that moments of the discretized solution, or equivalently its negative Sobolev norms (see remark below) can be addressed quite naturally.

Remark 3. The error estimate (17) can equivalently be written in terms of negative Sobolev norms. Let us define $H^{-s}(\mathbb{R})$ as the dual to $H^s(\mathbb{R})$ for $s \geq 0$ equipped with the norm [1]

$$\|u\|_{-s} = \sup_{g \in H^s} \frac{\left| \int g(x)u(x)dx \right|}{\|g\|_s}. \tag{18}$$

Then we can rewrite (17) in the more compact form

$$\|U - U_h\|_{-s} \leq Ch^{\frac{2(s+t)}{3}} \|g\|_t. \tag{19}$$

One advantage of using negative Sobolev spaces is precisely that

$$\left| \int p(x)(U_h(x) - U(x))dx \right| \leq \|U_h - U\|_{-s} \|p\|_s,$$

which, combined with (19), yields back (17).

Remark 4. The cases $\alpha = 0$ and $\alpha = 1$, corresponding to $\mu = \nu$, and $\mu = 0$ and $\nu = 1$, respectively, are trivial. For $\alpha = 0$, we have $R = e^{ih\xi}$, and for $\alpha = 1$, $R = 1$. These correspond exactly to the Fourier multiplier of the exact solution for $n = k/N$. Therefore, the method is *exact* for $\alpha = 0$ and $\alpha = 1$. This remark is quite important, for when the spatial discretization is adapted to the direction β, i.e. when the discretization cells are of the form $h_x \times h_y$ where $h_x/\mu = h_y/\nu$, DD does not create any spurious oscillations since $\alpha = 0$. The very reason that the discretization cannot always be adapted to the direction β in practice is that the transport equation involves the solution of many equations of the form (1) corresponding to different values of β and most resolution techniques require that the spatial discretization be the same for all directions [9,17].

Proof of Theorem 1. The proof of (15) is clear from Equations (12) and (13), and from the Parseval identity. The proof of the error estimate comes from the analysis of the behavior of the phase in (12) as $h \to 0$. We introduce

$$\psi(h\xi) = \frac{1}{h\xi}\theta(h\xi) - \frac{\mu}{\nu}. \tag{20}$$

Then we have

$$U_h(x) - U(x) = \frac{1}{2\pi} \int e^{-i\left(x - \frac{\mu}{\nu}\right)\xi} \left(e^{i\psi(h\xi)\xi} - 1\right)\hat{g}(\xi)d\xi. \tag{21}$$

Since $\mu/\nu = (1-\alpha)/(1+\alpha)$, we get that

$$\psi(h\xi) = \frac{1}{h\xi}\theta(h\xi) - \frac{1-\alpha}{1+\alpha}.$$

The asymptotic expansion of $\psi(h\xi)$ shows that

$$\psi(h\xi) = \frac{-1}{3}\frac{\alpha(\alpha-1)}{(1+\alpha)^3}(h\xi)^2 + O((h\xi)^4). \tag{22}$$

Denote by $b = \frac{-1}{3}\frac{\alpha(\alpha-1)}{(1+\alpha)^3}$, we obtain that

$$e^{i\psi(h\xi)\xi} - 1 = ibh^2\xi^3 + O(h^4|\xi|^5).$$

According to (14), the H^t norm of the difference $U_h - U$ squared is given by

$$\int \left|e^{i\psi(h\xi)\xi} - 1\right|^2 (1+|\xi|^2)^t |\hat{g}(\xi)|^2 d\xi.$$

We split this integral into two contributions I_1 and I_2, corresponding to $|\xi| < R$ and $|\xi| > R$, respectively, for $R > 0$ to be determined, but such that $h^4R^5 << 1$. The first contribution I_1 is bounded by

$$\begin{aligned}|I_1| &\le \int_{|\xi|<R} Ch^4|\xi|^{6-2(s-t)}(1+|\xi|^2)^s|\hat{g}(\xi)|^2 \\ &\le Ch^4R^{6-2(s-t)}\|g\|_s^2.\end{aligned}$$

The second contribution, in which $|e^{i\psi(h\xi)\xi} - 1|$ is bounded by 2, yields

$$|I_2| \le \int_{|\xi|>R} 2|\xi|^{-2(s-t)}(1+|\xi|^2)^s|\hat{g}(\xi)|^2 \le CR^{-2(s-t)}\|g\|_s^2.$$

Choosing $R = h^{-2/3}$ shows that both $|I_1|$ and $|I_2|$ are bounded by $Ch^{4(s-t)/3}$. Taking the square root of this estimate yields (16).

The estimate for the moments is proved similarly. Notice that

$$\int p(x)(U_h(x) - U(x))dx = \frac{1}{2\pi}\int e^{i\frac{\mu}{\nu}\xi}\Big(e^{i\psi(h\xi)\xi} - 1\Big)\hat{g}(\xi)\hat{p}(\xi)d\xi,$$

where $\hat{p}(\xi)$ is the Fourier transform of $p(x)$. We again split this integral into two contributions I_1 and I_2, corresponding to $|\xi| < R$ and $|\xi| > R$, with R to be determined. We obtain that

$$\begin{aligned}|I_1| &\le \frac{1}{2\pi}\int_{|\xi|<R} Ch^2|\xi|^{3-s-t}(1+|\xi|^2)^{s/2}\hat{g}(\xi)(1+|\xi|^2)^{t/2}\hat{p}(\xi)d\xi \\ &\le Ch^2R^{3-s-t}\|g\|_s\|p\|_t,\end{aligned}$$

by the Cauchy-Schwarz inequality. The other contribution is treated as follows

$$|I_2| \leq \frac{1}{2\pi}\int_{|\xi|>R} |\hat{g}(\xi)|\,|\hat{p}(\xi)|d\xi \leq CR^{-s-t}\|g\|_s\|p\|_t.$$

Choosing again $R = h^{-2/3}$ yields that both contributions $|I_1|$ and $|I_2|$ are bounded by $O(h^{2/3(s+t)})$. This concludes the proof of the theorem. $\square$

4. Local error estimates

We now want to have a better control on the location and amplitude of the oscillations created by DD. To this aim, we analyze the behavior of U_h for boundary conditions of the form $g(x) = \delta_x$ and $g(x) = H(x)$, where $H(x)$ is the Heaviside function defined by

$$H(x) = \begin{cases} 1 & \text{for } x \geq 0, \\ 0 & \text{for } x < 0. \end{cases} \tag{23}$$

Throughout this section, we assume that $\mu < \nu$. The results also hold for $\nu < \mu$, with μ/ν and ν/μ to be replaced by ν/μ and μ/ν, respectively. It is more convenient to analyze the problem using the discrete Fourier transform. Let us define $u_k^n = U^n(x - kh)$. We can then recast (6) as

$$u_k^{n+1} = \sum_{m=0}^{\infty} \alpha_m u_{k-m}^n, \tag{24}$$

for some real coefficients α_m. Let us assume that the coefficients u_k^n are the Fourier coefficients of $\hat{u}^n(\xi)$,

$$\hat{u}^n(\xi) = \sum_{k=-\infty}^{\infty} u_k^n e^{ik\xi}. \tag{25}$$

We obtain that

$$\hat{u}^{n+1}(\xi) = R(\xi)\hat{u}^n(\xi) = R^{n+1}(\xi)\hat{u}^0(\xi),$$

where $R(\xi)$ is defined in (10). Therefore, we have

$$U^n(x) = \sum_{m=0}^{\infty} c_m^n g(x - mh), \tag{26}$$

where

$$c_m^n = \frac{1}{2\pi}\int_{-\pi}^{\pi} e^{i[n\theta(u) - mu]}du.$$

On the upper edge of Ω, we have $n = h^{-1}$. We denote by $c_m = c_m^{h^{-1}}$.

Let us assume that $g(x) = \delta_x$. In the discrete case, this corresponds to $g(kh) = h^{-1}\delta_k$. Therefore, we see that the discrete and exact solutions are given by

$$U_h(kh) = h^{-1}c_k \qquad \text{and} \qquad U(x) = \delta(x - \mu/\nu). \tag{27}$$

The case $g(x) = H(x)$ is given by

$$U_h(kh) = \sum_{m=0}^{k} c_m \qquad \text{and} \qquad U(x) = H(x - \frac{\mu}{\nu}). \tag{28}$$

Notice that by Inverse Fourier transform, $\sum_{j=0}^{\infty} c_j = 1$ since $R(1) = 1$. Therefore we write the error $U_h(x) - U(x)$ as

$$U_h(x) - U(x) = \sum_m c_m[g(x - mh) - g(x - \frac{\mu}{\nu})]. \tag{29}$$

Hence, for $g(x) = H(x)$, we have

$$U_h(x) - U(x) = \sum_{mh \geq x - \mu/\nu} c_m \; - \sum_{mh < x - \mu/\nu} c_m. \tag{30}$$

The analysis of both (27) and (30) relies on a careful study of the Fourier coefficients c_k. Most of the results we need have been obtained by Hedstrom [11].

The main difficulty in the analysis is that $\theta(u)$ is real; hence the diamond scheme does not damp high frequencies. This makes the discretization scheme rather unstable as we will see. We want to obtain estimates for the coefficients c_m as $h \to 0$. These estimates depend on the form of the phase θ and the gain function R. Let us begin with some properties satisfied by R and θ. For a complex number $z = a + ib$, R is defined as

$$R(z) = \frac{\alpha + e^{ia}e^{-b}}{1 + \alpha e^{ia}e^{-b}}.$$

Therefore R is analytic in the half plane $b > \ln\alpha$ since $0 < \alpha < 1$ [10]. So $\theta = log(R)$ can be chosen analytic on $-\pi < u < \pi$. Let us state the following properties of θ (see also Fig.1):

1. The derivative θ' is positive on $(-\pi, \pi)$, reaches its minimum μ/ν for $u = 0$, and reaches its maximum ν/μ for $u = \pm\pi$.
2. The second derivative θ'' is negative on $(-\pi, 0)$ and positive on $(0, \pi)$; hence vanishes at $u = 0$ and $u = \pm\pi$ only.

We begin with a useful lemma:

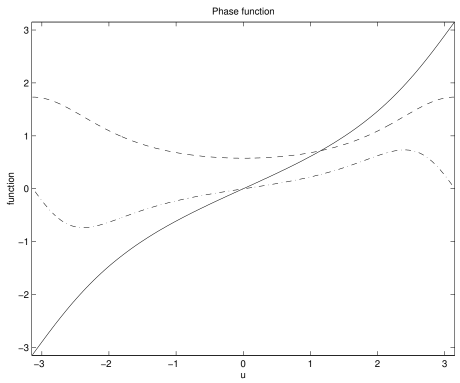

Fig. 1. Phase function $\theta(u)$ (solid), its first derivative (dashed), and second derivative (dashdot), for $\beta = \pi/3$.

Lemma 1. *Let $\phi_N(u)$ for $N \in \mathbb{N}^*$ be analytic functions on $(-\pi, \pi)$ with $\phi_N(\pi) = \phi_N(-\pi) + 2\pi$, and let $f(u)$ be a $2\pi-$periodic function of class $C^\infty(\mathbb{R})$. We further assume that*

$$|\phi'_N(u)| \geq \zeta(N) > 0 \quad \textit{for} \quad u \in \textit{Supp}(f)$$

and that all higher derivatives of ϕ_N are bounded independent of N. We want to estimate the following oscillatory integrals

$$\psi_N = \frac{1}{2\pi} \int_{-\pi}^{\pi} f(u) e^{iN\phi_N(u)} du.$$

Let us assume that $\varepsilon_N = \sum_{k=1}^{2} 1/(\zeta^k(N)N) \to 0$ when $N \to \infty$. Then $\psi_N = O(\varepsilon_N^\infty)$.

The notation $O(h^\infty)$ stands for a quantity satisfying $|O(h^\infty)| \leq C_k h^k$ for all $k \in \mathbb{N}$ and some constants C_k independent of h.

Proof. We have for all k

$$\psi_N = \frac{1}{2\pi} \int_{-\pi}^{\pi} f(u) \Big(\frac{1}{iN\phi'_N(u)} \frac{d}{du} \Big)^k e^{iN\phi_N(u)} du.$$

By integration by parts and periodicity, we obtain that

$$\psi_N = \frac{1}{2\pi} \int_{-\pi}^{\pi} \sum_{l=k}^{2k} f_{k,l}(u) \frac{1}{N^k (\phi'_N(u))^l} e^{iN\phi_N(u)} du,$$

where the functions $f_{k,l}(u)$ and sums of products of derivatives of $f(u)$ and of $\phi''_N(u)$; hence $f_{k,l}(u) \in C^\infty(\mathbb{R})$ and $\mathrm{Supp}(f_{k,l}) \subset \mathrm{Supp}(f)$. Therefore, we deduce the existence of constants C_k such that

$$|\psi_N| \leq \frac{C_k}{N^k} \Big(\frac{1}{\zeta^k(N)} + \frac{1}{\zeta^{2k}(N)} \Big).$$

This concludes our proof. □

We deduce from this lemma that the important contribution in the coefficients c_m arises from those points $u \in (-\pi,\pi)$ close to a point of singularity of the phase $h^{-1}\theta(u) - mu$, that is to say a point satisfying $h^{-1}\theta'(u) = m$. For instance, we have

Lemma 2. *Let $\varepsilon > 0$. The coefficients c_m such that $mh > \nu/\mu + h^{1/2-\varepsilon}$ or $mh < \mu/\nu - h^{1/2-\varepsilon}$ satisfy*

$$c_m = O\Big(\Big[\frac{h}{1+mh}\Big]^\infty\Big).$$

Proof. The proof is a direct application of Lemma 1 by choosing $\phi_N(u) = \theta(u) - (m/N)u$ with $\zeta(N) = N^{-1/2+\varepsilon}$ (recall that $h = N^{-1}$) and remarking that $\mu/\nu \le \theta'(u) \le \nu/\mu$. □

We treat the other coefficients c_m as follows. Let us first define u_m as the point in $(0,\pi)$ such that $\theta'(u_m) = hm$ for the values of m satisfying $\mu/\nu \le mh \le \nu/\mu$, $u_m = \pi$ for those values of m such that $mh \le \nu/\mu$, and $u_m = 0$ for those values of m such that $\mu/\nu \le mh$. Notice that $\theta'(-u_m) = \theta'(u_m)$.

We now define the functions η_m, whose role is to restrict $(-\pi,\pi)$ to a smaller subdomain of point u that contribute to the coefficient c_m. For m such that $|mh - \mu/\nu| \ge \delta$, we denote by η_m a $2\pi-$periodic function of class $C^\infty(I\!R)$ such that $0 \le \eta_m(u) \le 1$, $\eta_m(u) = 1$ for $|u \pm u_m| < \delta/3$, and $\eta_m(u) = 0$ for $|u \pm u_m| \ge \delta$. For m such that $|mh - \mu/\nu| < \delta$, we denote by $\eta_m(u)$ a $2\pi-$periodic function of class $C^\infty(I\!R)$ such that $0 \le \eta_m(u) \le 1$, $\eta_m(u) = 1$ for $|u - \mu/\nu| < 3\delta/2$, and $\eta_m(u) = 0$ for $|u - \mu/\nu| \ge 2\delta$.

We introduce

$$d_m = \frac{1}{2\pi}\int_{-\pi}^{\pi} \eta_m(u) e^{i[h^{-1}\theta(u) - mu]} du.$$

Using Lemma 1, we deduce that $c_m = d_m + O(h^\infty)$. It remains to estimate the contributions d_m. This is done by using the results in Lemmas 9.2 and 9.5 of [11].

Lemma 3. *We treat three cases, corresponding to points u_m close to 0, close to π, or away from those two values.*

- *Let m be such that $\mu/\nu - h^{1/2-\varepsilon} \le mh \le \mu/\nu + \delta$ and define $\omega = mh - \mu/\nu$. Then for every positive M, we have*

$$|c_m| \le C_M h^{1/3}, \qquad |\omega| \le M h^{2/3}.$$

There exists ω_0 such that

$$|c_m| \le C h^3, \qquad \omega_0 \le \omega \le \delta.$$

There exist smooth functions g_m, $\tilde{g}_m$, and h_m such that

$$c_m = g_m(\omega)\exp\left(\frac{ih_m(\omega)}{h}\right)+\tilde{g}_m(\omega)\exp\left(\frac{-ih_m(\omega)}{h}\right)+Q(m,\omega), \quad h^{2/3} \le \omega \le \omega_0,$$

with $|Q(m,\omega)| \le Ch^{1/2}\omega^{-1/4}\exp(-\kappa h^{-1}\omega^{3/2})+Ch^3$ *for some* $\kappa > 0$. *The functions* g_m *and* $\tilde{g}_m$ *are bounded by* $Ch^{1/2}\omega^{-1/4}$.

- *Let m be such that $mh > \mu/\nu + \delta$. Let $r_m = 1$ for m such that $\eta_m(\pi) = 0$ and $r_m = 2$ for m such that $\eta_m(\pi) = 1$. Let us define $\omega = mh - \theta'(u_m)$ and $\omega_0 = \max_u |\theta'(u) - \theta'(u_m)|$. Then we have*

$$|c_m| \le \begin{cases} Ch^{1/(r_m+1)} & |\omega| \le h^{r_m/(r_m+1)} \\ Ch^{1/2}|\omega|^{(r_m-1)/(2r_m)} & h^{r_m/(r_m+1)} \le |\omega| \le \omega_0. \end{cases}$$

Remark 5. This lemma shows the following. The coefficients c_m are of order $h^{1/2}$ except for those values of m such that u_m is close to 0 or π. When u_m is close to π, the coefficients are of order $h^{1/3}$ on a small interval of length $h^{2/3}$ and then decay exponentially when u_m moves away from π, until they become of order $h^{1/2}$.

The coefficients c_m for u_m close to 0 have a more complicated behavior. They are of size $h^{1/3}$ over a large interval, but have fast oscillations. Those oscillations are well approximated by the Airy function [12], which appears in a similar context in the propagation of dispersive waves [23].

A numerical experiment for the coefficients $h^{-1}c_m$ with $\beta = \pi/3$ and $N = 200$ is given in Fig. 2. The coefficients are not negligible only in the region ($\mu/\nu \approx 0.5774, \nu/\mu \approx 1.7321$) as prescribed by theory. We see how the exact solution (a delta function at $x = \mu/\nu$) is dispersed by DD. Notice that this dispersion is very anisotropic. The solution is exponentially small on the left of the support of the exact solution $x = \mu/\nu$, very oscillatory on its right up to the point ν/μ, and again exponentially small for $x > \nu/\mu$. This highly oscillatory pattern on a finite interval does not seem to have been observed elsewhere.

Let us now turn to the case of a step function boundary condition $g(x) = H(x)$. The error $Y(x) = U_h(x) - U(x)$ is given by (30). We therefore have to estimate the sum of the coefficients c_m. We actually deduce that the contribution of the terms such that $mh < \mu/\nu$ is small according to Lemma 2. The estimation of the sum of the coefficients c_m is non trivial because of the oscillations reported in Lemma 3. We deduce from the Remark at the end of §9 in [11] and from Lemma 2 the following result

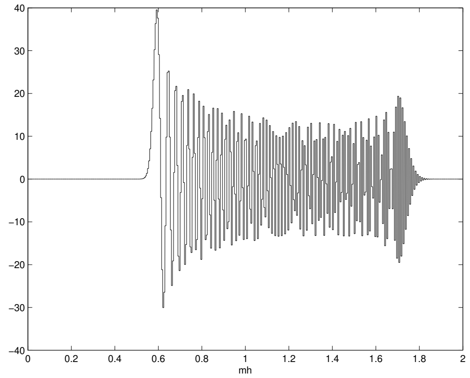

Fig. 2. Coefficients Nc_m, for $N = 200$ and $\beta = \pi/3$.

Lemma 4. *Let ω_0 as in Lemma 3. The error $Y(x)$ satisfies*

$$|Y(x)| \leq \begin{cases} C & |x - \dfrac{\mu}{\nu}| \leq h^{2/3}, \\ Ch^{1/2}|x - \dfrac{\mu}{\nu}|^{-3/4} & h^{2/3} < |x - \dfrac{\mu}{\nu}| \leq \omega_0, \\ Ch^{1/2} & \omega_0 \leq |x - \dfrac{\mu}{\nu}| \leq \dfrac{\nu}{\mu} - \dfrac{\mu}{\nu} + h^{1/2-\varepsilon}, \\ O(h^\infty) & |x - \dfrac{\mu}{\nu}| > \dfrac{\nu}{\mu} - \dfrac{\mu}{\nu} + h^{1/2-\varepsilon}. \end{cases}$$

We deduce from the lemma that $\|Y\|_{L^1(\mathbb{R})} = O(h^{1/2})$. Integrating separately the four contributions of $Y(x)$, we obtain more generally that

$$\|Y\|_{L^p(\mathbb{R})} = \|U - U_h\|_{L^p(\mathbb{R})} \leq C_p \begin{cases} h^{1/2} & 1 \leq p \leq \frac{4}{3} \\ h^{2/(3p)} & \frac{4}{3} \leq p \leq \infty. \end{cases} \qquad (31)$$

For $p = 2$, we recover the same error estimate $h^{1/3}$ as in Theorem 1 with $s = 1/2$ and $t = 0$ (recall that step functions are *almost* in $H^{1/2}$. Both solutions $U(x)$ and $U_h(x)$ are given in Fig. 3 for $N = 200$ and $\beta = \pi/3$. Observe again the anisotropy of the oscillations. The solution is almost exact on the left of the discontinuity point $x = \mu/\nu$ and on the right of the point $x = \nu/\mu$, and highly oscillatory in between.

5. Dissipative case

Let us now come back to the general case $\gamma \geq 0$. The multiplication in Fourier space (9) is valid, with $R(h\xi) = R_\gamma(h\xi)$ now depending on

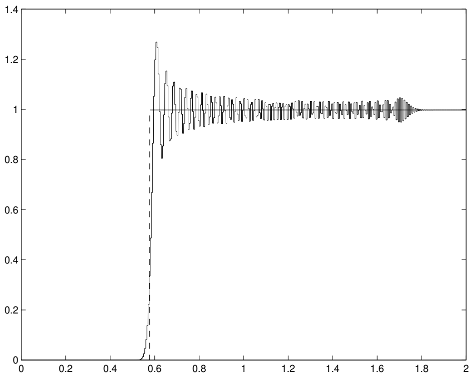

Fig. 3. Solutions $U_h(x)$ (solid) and $U(x)$ (dashed), for $N = 200$ and $\beta = \pi/3$.

γ. We introduce

$$\alpha = \frac{\nu - \mu}{\nu + \mu}, \qquad \beta = \frac{\gamma}{2(\mu + \nu)}, \qquad \eta(h\xi) = \beta \frac{1 + e^{ih\xi}}{\alpha + e^{ih\xi}}. \tag{32}$$

After some algebra, we obtain the following form for R_γ:

$$R_\gamma(h\xi) = R_0(h\xi) \frac{1 - \eta(h\xi)h}{1 + R_0(h\xi)\eta(h\xi)h} \equiv R_0(h\xi) S_\gamma(h\xi). \tag{33}$$

We can check that $|1 - \eta(h\xi)h| \leq 1$ and $|1 + R_0(h\xi)\eta(h\xi)h| \geq 1$. Therefore, $|R_\gamma(h\xi)| \leq 1$ and the problem is well posed in L^2. Notice that for $h\xi = (2k+1)\pi$, $\eta(h\xi) = 0$ and $|R_\gamma(h\xi)| = 1$. Therefore, some high frequencies are not absorbed at all by the diamond discretization. We will see that this property causes a lot of damage for non smooth boundary conditions.

The discrete and exact solutions to (1) are given by

$$U_h(x) = \frac{1}{2\pi} \int e^{-ix\xi} S_\gamma(h\xi)\ e^{ih^{-1}\theta(h\xi)}\ \hat{g}(\xi) d\xi \tag{34}$$

$$U(x) = \frac{1}{2\pi} \int e^{-ix\xi} e^{i\frac{\mu}{\nu}\xi - \frac{\gamma}{\nu}}\ \hat{g}(\xi) d\xi = e^{-\frac{\gamma}{\nu}} g(x - \frac{\mu}{\nu}). \tag{35}$$

We show the following result.

Theorem 2. *We assume that $\mu \neq \nu$, $\nu > 0$, and $\gamma > 0$. Let $g \in H^s(\mathbb{R})$. Then $U(x) \in L^2(\mathbb{R})$, $U_h(x) \in L^2(\mathbb{R})$, and*

$$\|U_h\| \leq \|g\| = e^{\gamma/\nu} \|U\|. \tag{36}$$

Assume that for some ε, $h^\varepsilon \gamma^2 << 1$. For $0 \leq t \leq s \leq 3$, we have

$$\|U_h - U\|_t \leq CG(\gamma, h, s, t) \|U\|_s, \tag{37}$$

where

$$G(\gamma,h,s,t)=\min\Big(e^{\frac{\gamma}{\nu}}h^{\frac{2(s-t)}{3}},\ \max(1,\ e^{\frac{\gamma}{\nu}}h^{s-t})\Big).$$

Moreover, let $g\in H^t(\mathbb{R})$ and $p\in H^s(\mathbb{R})$. Then the moments of the convection equation satisfy the following estimate, for $s\geq 0$ and $t\geq 0$ such that $t+s\leq 3$,

$$\Big|\int p(x)(U_h(x)-U(x))dx\Big|\leq CG(\gamma,h,s,-t)\|U\|_t\|p\|_s. \tag{38}$$

Remark 6. The estimates of this theorem can be interpreted as follows. When the absorption γ is small enough, the DD scheme behaves as in the conservative case. For instance, for $s=1/2$ and $t=0$, corresponding to the L^2 norm of the error for a piecewise constant boundary condition, we have an error of order $h^{1/3}$ independently of γ for γ small enough.

When γ is large, the exponential factor becomes predominant, and the term $e^{\gamma/\nu}h^{2/3(s-t)}$ becomes larger than 1 unless γ is very small. In this case, the DD scheme is not a good approximation of the exact solution. However, it turns out that it behaves a little better than $e^{\gamma/\nu}h^{2/3(s-t)}$, as $e^{\gamma/\nu}h^{s-t}$. So for $s=1/2$ and $t=0$, when absorption is large, the L^2 norm is not well approximated by DD, but as h goes to 0, the error behaves like $e^{\gamma/\nu}h^{1/2}$ as long as it is larger than unity.

We have a similar result for the critical directions corresponding $\mu=\nu$, and $\mu=0$, that is to say when the spatial discretization is adapted to the direction of propagation β (see remark 4).

Theorem 3. *Assume that $\mu=\nu$, i.e., $\beta=\pi/4$, or that $\mu=0$, i.e., $\beta=0$. With the assumptions of Theorem 2, the results (37) and (38) hold with $G(\gamma,h,s,t)$ replaced by*

$$G_{\mu=\nu}(\gamma,h,s,t)=e^{\frac{\gamma}{\sqrt{2}}}h^{s-t},\qquad \textit{and}\qquad G_{\mu=0}(\gamma,h,s,t)=\gamma^3e^{\gamma}h^2, \tag{39}$$

for $\mu=\nu$ and $\mu=0$, respectively.

Proof of Theorem 2. The difference U_h-U is given by

$$\begin{aligned}U_h(x)-U(x)&=\frac{1}{2\pi}\int e^{-ix\xi}(S_\gamma^N(h\xi)e^{ih^{-1}\theta(h\xi)}-e^{(i\mu\xi-\gamma)/\nu})\hat{g}(\xi)d\xi\\&=\frac{1}{2\pi}\int e^{-ix\xi}\Big(e^{i\psi(h\xi)\xi}e^{\frac{\gamma}{\nu}}S_\gamma^N(h\xi)-1\Big)\hat{U}(\xi)d\xi,\end{aligned} \tag{40}$$

where $N = h^{-1}$. We know from (22) the behavior of $\psi(h\xi)\xi$ for ξ close to 0. It remains to obtain an estimate of order h^2 for $e^{\gamma/\nu} S_\gamma^N(h\xi)$ and show how it degrades when γ becomes large (but still independent of h); hence we need to control the order h^2 of the estimate. After some asymptotic expansions, we obtain that

$$S_\gamma^N = e^{-(1+R_0)\eta}\Big(1 + \frac{\eta^2(R_0^2-1)}{2N} + \frac{\eta^3}{24N^2}\Big[-8(1+R_0^2) + 3\eta(1-R_0^2)^2\Big]\Big) + O(\frac{1}{N^3}).$$

We have that $\eta(h\xi) = \gamma/[(1+\alpha)(\mu+\nu)] + O(h\xi)$. Since $R_0(h\xi) = 1 + O(h\xi)$, we deduce that

$$e^{\dfrac{\gamma}{\nu}} S_\gamma^N(h\xi) = e^{\dfrac{\gamma}{\nu} - (1+R_0)\eta}(1 + O(\gamma^2 h^2 \xi) + O(\gamma^3 h^2)) \tag{41}$$

provided $h|\xi| < C$. It remains to find the asymptotic expansion of $e^{\gamma/\nu - (1+R_0)\eta}$, which is given, using the fact that $4\beta/(1+\alpha) = \gamma/\nu$, by

$$e^{\dfrac{\gamma}{\nu} - (1+R_0)\eta} - 1 = \frac{\gamma}{\nu}\frac{(1-\alpha)^2}{4(1+\alpha)^2}(h\xi)^2 + O(\gamma h^3 \xi^3).$$

This expansion holds provided that $\gamma h^2|\xi|^2 << 1$. When ξ grows much larger, $\eta(h\xi)$ can vanish and this expression is bounded by $e^{\gamma/\nu}$ only.

The coefficient $\left|e^{i\psi(h\xi)\xi} e^{\gamma/\nu} S_\gamma^N(h\xi) - 1\right|$ in (40) is therefore of order $O(1+\gamma^3)O(h^2|\xi^3|)$ when $h^4|\xi|^5 << 1$. We can see that it is bounded by a constant times $1+\gamma^3$ when $\gamma h^2|\xi|^2 << 1$. When $|\xi|$ becomes larger, this quantity is bounded by $e^{\gamma/\nu}$ only. The coefficient $1+\gamma^3$ is not necessarily optimal. However it is negligible compared with $e^{\gamma/\nu}$. Let us summarize these bounds:

$$\left|e^{i\psi(h\xi)\xi} e^{\dfrac{\gamma}{\nu}} S_\gamma^N(h\xi) - 1\right| \le \begin{cases} C(1+\gamma^3)h^2|\xi|^3 & \text{when } h^4|\xi|^5 << 1 \\ C(1+\gamma^3) & \text{when } \gamma h^2|\xi|^2 << 1 \\ Ce^{\dfrac{\gamma}{\nu}} & \text{always.} \end{cases} \tag{42}$$

We now follow the proof of Theorem 1. The H^t norm of the difference $U_h - U$ squared is given by

$$I = \int \left|e^{i\psi(h\xi)\xi} e^{\dfrac{\gamma}{\nu}} S_\gamma^N(h\xi) - 1\right|^2 (1+|\xi|^2)^t |\hat{U}(\xi)|^2 d\xi.$$

We split the integral into the same contributions I_1 and I_2, corresponding to $|\xi| < R$ and $|\xi| > R$, respectively. As in the proof of Theorem 1, we obtain using the bounds in (42),

$$\frac{I_1}{\|U\|_s^2} \leq \begin{cases} C(1+\gamma^3)^2 h^4 R^{6-2(s-t)} & \text{if } h^2R^3 << 1 \\ C(1+\gamma^3)^2 & \text{if } \gamma h^2 R^2 << 1 \end{cases}, \quad \frac{I_2}{\|U\|_s^2} \leq Ce^{\dfrac{2\gamma}{\nu}} R^{-2(s-t)}.$$

Consider now two cases. We first choose $R = h^{-2/3}$ as in the conservative case. Then, I_1 is bounded by $C(1+\gamma^3)h^{4/3(s-t)}$ and I_2 is bounded by $Ce^{2\gamma}\nu h^{4/3(s-t)}$. Therefore, we obtain that

$$I \leq Ce^{\dfrac{2\gamma}{\nu}} h^{\dfrac{4}{3}(s-t)} \|U\|_s^2.$$

When γ is not too large, the accuracy of DD is the same whether there is absorption or not. When the absorption γ is very large, this bound becomes larger than 1 and is actually not optimal anymore. The reason is that the above estimate relies on the smallness of $h^2|\xi|^3$ to show that Diamond Discretization correctly approximates the low frequencies. When absorption becomes large, the optimal radius is not as above, but rather

$$R = h^{-1+\varepsilon},$$

where ε is arbitrarily small provided $\gamma h^{2\varepsilon} << 1$. For values of ξ below this radius, the kernel R_0 is not well approximated, so the error will remain of order 1. However, the absorption kernel $e^{\gamma/\nu-(1+R_0)\eta}$ remains bounded independently of γ. So I_1 will remain bounded by $C(1+\gamma^3)$, whereas I_2 will be of the form $e^{2\gamma}\nu h^{2(s-t)(1-\varepsilon)}$. We conclude that

$$I \leq \max(C, Ce^{\dfrac{2\gamma}{\nu}} h^{2(s-t)(1-\varepsilon)}) \|U\|_s^2.$$

The estimate for the moments is obtained similarly. This concludes the proof of the theorem. □

Proof of Theorem 3. The proof is similar to that of Theorem 2. We use the same notation. Consider first the case $\mu = \nu = \sqrt{2}$. This yields $\alpha = 0$, and $R_0(h\xi) = e^{ih\xi}$. Therefore, following the proof of Theorem 2, the bound (42) can be replaced by

$$\left| e^{\dfrac{\gamma}{\nu}} S_\gamma^N(h\xi) - 1 \right| \leq \begin{cases} C(1+\gamma^3)h^2|\xi|^2 & \text{when } h|\xi| < C \\ Ce^{\dfrac{\gamma}{\sqrt{2}}} & \text{always.} \end{cases} \tag{43}$$

It remains to choose $R = h^{-1}$ in the computation of the integral I to obtain the theorem.

The case $\mu = 0$ is even simpler. Here, $R_0 = 1$, $\alpha = 1$, and $\eta = \gamma/(2\nu) = \gamma/2$. So the error kernel in Fourier domain is given by

$$e^{\gamma} R_{\gamma}^{N} - 1 = e^{\gamma}\Big(\frac{1-\eta h}{1+\eta h}\Big)^{N} - 1 = \frac{1}{12} e^{\gamma}\gamma^{3} h^{2} + O(h^{4}).$$

This proves the theorem. □

We now give some more local information on the incorrect damping of some high frequencies. We consider the boundary conditions $g = \delta$ and $g = H$ as in section 4. We also assume that $\mu < \nu$ to simplify. Let us rewrite (26) as

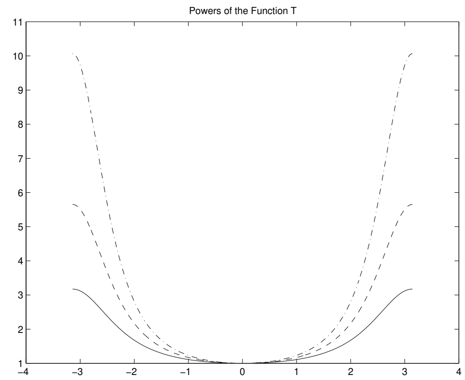

Fig. 4. Functions $T(u)$ (solid), $T^{3/2}(u)$ (dashed), and $T^{2}(u)$ (dotdash), for $\beta = \pi/3$.

$$U^{n}(x) = \sum_{m=0}^{\infty} c_{\gamma,m}^{n} g(x - mh), \tag{44}$$

where

$$c_{\gamma,m}^{n} = \frac{1}{2\pi}\int_{-\pi}^{\pi} R_{\gamma}^{n}(u) e^{-imu} du.$$

We also denote by $c_{\gamma,m} = c_{\gamma,m}^{h^{-1}}$. We are interested in estimating $e^{\gamma/\nu}U^{n}(x)$, since $e^{\gamma/\nu}U(x) = g(x - \mu/\nu)$ is of order 1 independently of γ. We now estimate the leading term of the coefficients $c_{\gamma,m}$ when $h \to 0$. From the proof of Theorem 2, we deduce that

$$e^{\gamma/\nu} c_{\gamma,m} = \frac{1}{2\pi}\int_{-\pi}^{\pi} e^{ih^{-1}\theta(u)} e^{\gamma/\nu - (1+R_0(u))\eta(u)} e^{-imu} du + O(h).$$

Let us analyze the term

$$e^{\gamma/\nu - (1+R_0(u))\eta(u)} = (e^{1/\nu - (1+R_0(u))\eta(u)/\gamma})^{\gamma} \equiv (T(u))^{\gamma}.$$

The function $T(u)$ is now independent of h and γ. After painful but easy calculations, we obtain

$$(1+R_0(u))\eta(u)/\gamma = \frac{(1+\alpha)^2}{4\nu}\frac{(1+\alpha)^2(1+2\cos u+\cos^2 u)+(1-\alpha)^2\sin^2 u}{(1+2\alpha\cos u+\alpha^2)^2}.$$

Notice that this quantity turns out to be real. We observe that it equals $1/\nu$ for $u=0$, and equals 0 for $u=\pm\pi$. Therefore, $T(0)=1$, which is good, but $T(\pm\pi)=e^{1/\nu}$, which means that the corresponding frequencies are not damped at all. The graph of the function T is represented for $\beta=\pi/3$ in Fig. 4.

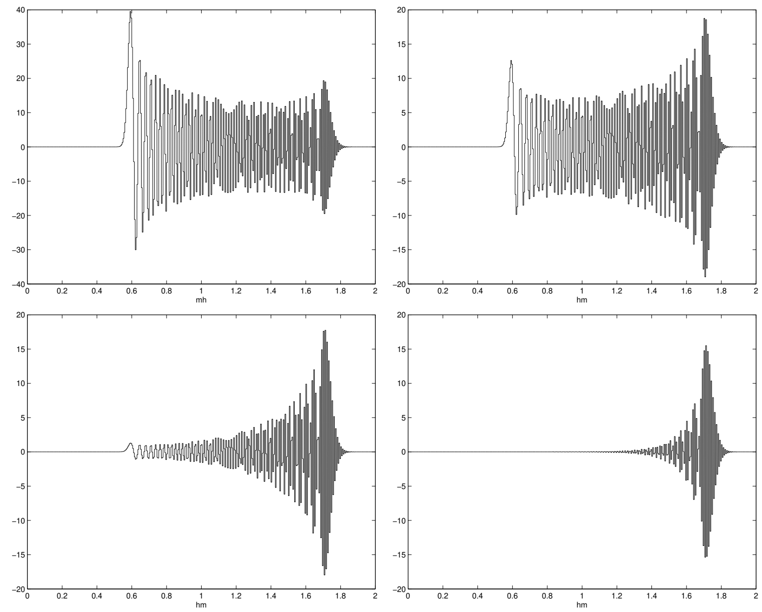

Fig. 5. Coefficients $Nc_{\gamma,m}$, for $N=200$, $\beta=\pi/3$ and different values of γ. Top left: $\gamma=0$; Top right: $\gamma=1$; Bottom left: $\gamma=3$; Bottom right: $\gamma=9$.

We know that the coefficient $c_{\gamma,m}$ mainly depends on the points u close to the point u_m such that $\theta'(u_m)=hm$, for m such that $\mu/\nu<hm<\nu/\mu$. Hence, we obtain that

$$e^{\gamma/\nu}c_{\gamma,m}\approx T^{\gamma}(u_m)\,c_m.$$

Therefore, the coefficients corresponding to small values of m are multiplied by $T(0) = 1$ and are correctly damped by the numerical scheme. The coefficients corresponding to $u_m \approx \nu/\mu$ however, are multiplied by $e^{\gamma/\nu}$, which can be fairly large even for moderate values of absorption. The coefficients $h^{-1}c_{\gamma,m}$ are represented in Fig. 5 for different values of γ. We see that the largest coefficients are of order h^{-1} for $u_m \approx \mu/\nu$ (left side of the oscillations) and $h^{-2/3}e^{\gamma/\nu}$ for $u_m \approx \nu/\mu$ (right side of the oscillations). These two terms are comparable for $\gamma \approx (\nu/3)\ln(h^{-1})$.

Since $T^\gamma(u_m)$ varies smoothly in u, the summation of the $c_{\gamma,m}$ can be performed as previously. This provides us with an estimate of the error for step function boundary condition. Denoting $Y_\gamma(x) = e^{\gamma/\nu}(U_h(x) - U(x))$, we have

$$|Y_\gamma(x)| \le T^\gamma((\theta')^{-1}(x))|Y(x)|, \qquad \text{for} \quad \frac{\mu}{\nu} < x < \frac{\nu}{\mu}, \tag{45}$$

where the bounds for $Y(x)$ are given in Lemma 4. Therefore, for x close to μ/ν, where $T^\gamma((\theta')^{-1}(x)) \approx 1$, the error $U_h(x) - U(x)$ is of order $e^{-\gamma/\nu}Y(x)$, which is relatively small. However, for x close to ν/μ, where $T^\gamma((\theta')^{-1}(x)) \approx e^{\gamma/\nu}$, the error $U_h(x) - U(x)$ is of order $Y(x)$, that is to say the same error in absolute value as when no absorption is present. We have represented $U(x)$ and $U_h(x)$ for different values of γ, $N = 200$ and $\beta = \pi/3$ in Fig.6. Notice that for large values of γ, we deduce from Lemma 4 and (45) that $|Y_\gamma(x)|$ is bounded by $Ce^{\gamma/\nu}h^{1/2}$. This is exactly the estimate provided by Theorem 2 for large γ, $s = 1/2$ and $t = 0$.

6. Two dimensional moment estimates

So far, we have analyzed the outgoing distribution $u_{|\Gamma_1}$ and its approximation by Diamond Discretization. In this section, we focus on estimates of the two-dimensional solution $u(x,y)$. The analysis in section 2 displayed the DD approximation of u at vertical coordinates of the form $y = nh$, where $n \in I\!N$. To analyze the two-dimensional solution $u(x,y)$, we need to interpolate between those vertical coordinates. We proceed as follows. Let us first denote by $U_h(x,y)$ the discretized solution. So far, we have that $U_h(x,nh) = U^n(x)$. We deduce from the results in section 2 that

$$\hat{U}_h(\xi, y) = (R(h\xi))^{y/h}\hat{g}(\xi), \tag{46}$$

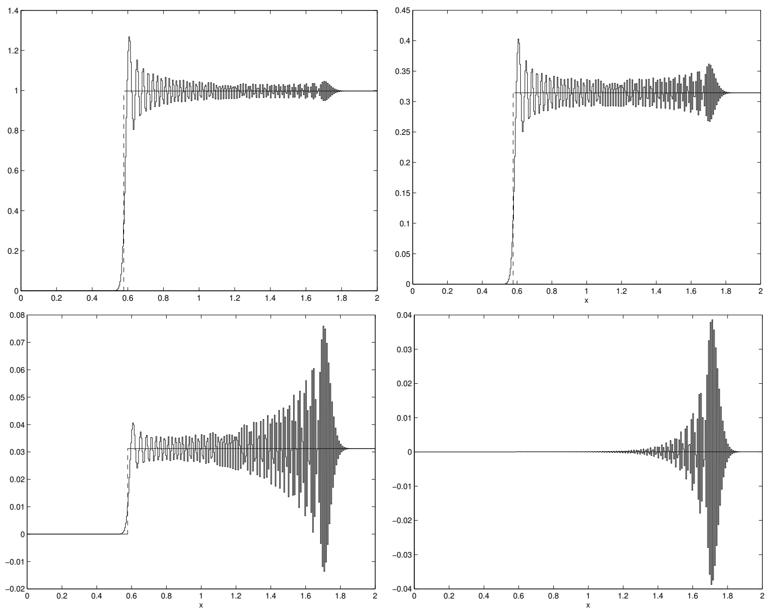

Fig. 6. Solutions $U_h(x)$ (solid) and $U(x)$ (dashed), for $N = 200$, $\beta = \pi/3$ and different values of γ. Top left: $\gamma = 0$; Top right: $\gamma = 1$; Bottom left: $\gamma = 3$; Bottom right: $\gamma = 9$.

for the coordinates $y = hn$ with $n \in \mathbb{N}$. We extend $U_h(\xi, y)$ given by (46) to all values of $y \in \mathbb{R}^+$. This yields the expression

$$U_h(x,y) = \frac{1}{2\pi} \int e^{-ix\xi} e^{i\frac{\theta(h\xi)}{h\xi} y\xi} \hat{g}(\xi) d\xi. \tag{47}$$

Let us assume that $\gamma = 0$ to simplify the presentation. We state the following result.

Theorem 4. *Assume that $\mu \neq \nu$ and $\nu > 0$. Let $g \in H^s(\mathbb{R})$. Then $U(x) \in L^2(\mathbb{R})$, $U_h(x) \in L^2(\mathbb{R})$, and*

$$\|U\| = \|U_h\| = \|g\|. \tag{48}$$

For all s, t, such that $0 \leq t \leq s \leq 3$, we have

$$\|U_h - U\|_t \leq Ch^{\frac{2(s-t)}{3}} \|g\|_s = Ch^{\frac{2(s-t)}{3}} \|U\|_s. \tag{49}$$

Moreover, let $g \in H^t(\mathbb{R})$, $p \in H^s(\mathbb{R})$ and $q \in L^\infty(\mathbb{R})$ such that its Fourier transform $\hat{q}(\zeta)$ is continuously differentiable on $\mathbb{R}$ and satisfies

$$|\hat{q}(\zeta)| \leq C|\zeta|^{-u}, \qquad |\hat{q}'(\zeta)| \leq C|\zeta|^{-v},$$

for some positive constants u and v. Then the moments of the convection equation satisfy the following estimate, for $s,t,u,v \geq 0$ such that $t+s+v \leq 3$,

$$\Big|\int p(x)q(y)(U_h(x,y)-U(x,y))dx\,dy\Big| \leq Ch^{\dfrac{2(s+t+u)}{3-v+u}}, \tag{50}$$

where the constant C depends on g, p, and q.

Remark 7. The estimate (50) can be used as follows. The Fourier transform of a step function $q(y)$ is of the form $\hat{q}(\zeta) = |\zeta|^{-1}(e^{iy_1\zeta} - e^{iy_2\zeta})$. Therefore, in the theorem, we have $u = v = 1$, and obtain

$$\Big|\int_0^L \int_{y_1}^{y_2} p(x)(U_h(x,y)-U(x,y))dx\,dy\Big| \leq Ch^{\dfrac{2(s+t+1)}{3}}. \tag{51}$$

Therefore, when $s+t+1 \leq 3$, the step integration in the second variable y yields an error for the moment $h^{2/3}$ more accurate than its local counterpart treated in Theorem 1. We will demonstrate this assertion numerically in the next section.

Proof of Theorem 4. The first part of the theorem is identical to that of Theorem 1. Let us now prove the estimate (50). We have by (47) and the Parseval identity that

$$\int p(x)q(y)(U_h-U)(x,y)dx\,dy = \frac{1}{2\pi}\int \hat{g}(\xi)\hat{p}(\xi)[\hat{q}(\frac{\theta(h\xi)}{h\xi}\xi)-\hat{q}(\frac{\mu}{\nu}\xi)]d\xi.$$

We again split this integral into the two contributions I_1 and I_2 corresponding to $|\xi| < R$ and $|\xi| > R$, respectively.

Consider I_2 first. We check that $\mu/\nu \leq \theta(h\xi)/(h\xi) \leq \nu/\mu$. Therefore $|\theta(h\xi)/(h\xi)\xi|$ and $|\nu/\mu\xi|$ are larger than $C|\xi|$ for $|\xi| \geq R$ for a certain constant C independent of ξ and R large enough. Hence,

$$|I_2| \leq C\int |\xi|^{-(s+t+u)}(1+|\xi|^2)^{s/2}\hat{g}(\xi)(1+|\xi|^2)^{t/2}\hat{p}(\xi) \leq CR^{-(s+t+u)}\|g\|_s\|p\|_t.$$

We now treat the contribution I_1. We have that

$$\hat{q}(\frac{\theta(h\xi)}{h\xi}\xi) - \hat{q}(\frac{\mu}{\nu}\xi) = (\frac{\theta(h\xi)}{h\xi}\xi - \frac{\mu}{\nu}\xi)\hat{q}'(\xi_1(\xi)),$$

with $\xi_1(\xi)$ between $\frac{\theta(h\xi)}{h\xi}\xi$ and $\frac{\mu}{\nu}\xi$. Therefore, $\mu/\nu\xi \leq \xi_1(\xi) \leq \nu/\mu\xi$. We deduce from the hypotheses that $|\hat{q}'(\xi_1(\xi))| \leq C|\xi|^{-v}$. We already know from the proof of Theorem 1 that $|\frac{\theta(h\xi)}{h\xi}\xi - \frac{\mu}{\nu}\xi| \leq Ch^2|\xi|^3$. Therefore,

$$\begin{aligned}|I_1| &\leq C\int h^2|\xi|^{3-(s+t+v)}(1+|\xi|^2)^{s/2}\hat{g}(\xi)(1+|\xi|^2)^{t/2}\hat{p}(\xi)\\ &\leq Ch^2R^{-(s+t+v)}\|g\|_s\|p\|_t.\end{aligned}$$

Choosing $R = h^{-2/(3-v+u)}$ in both contributions yields the theorem.
□

7. Numerical simulations

This section is devoted to the numerical validation of the error estimates given in the preceding sections. The computations are performed by using the DD discretization given by (3), which is the algorithm implemented in practice.

The boundary condition is $U_h(x, y = 0) = g(x)$. It is constant on each edge of the discretization $((k-1)h, kh)$. For each $y = nh$, and $x \in ((k-1)h, kh)$, we have $U_h(x, y) = U_k^n$, where U_k^n is obtained by solving (3). The solution of DD in the volume is given, for $nh < y < n(h+1)$ by

$$\bar{U}_h(x,y) = \frac{1}{2}(U_k^n + U_k^{n+1}). \tag{52}$$

We have analyzed $U_h(x, 1)$ in sections 3, 4, and 5. The theoretical analysis of these sections differs slightly from the numerical implementation in the sense that the numerical boundary condition $g(x)$ is now piecewise constant. However, we will see that the theoretical estimates still hold for this implementation of Diamond Discretization. We have analyzed $\bar{U}_h(x, y)$ in section 6. The function $U_h(x, y)$ defined in section 6 was given by a different interpolation from (52) for the values of the vertical coordinate $nh < y < (n+1)h$. The midpoint integration rule used in (52) is however known to be of accuracy h^2. Therefore, both $U_h(x, y)$ and $\bar{U}_h(x, y)$ have the same accuracy as $h \to 0$.

Conservative Case. We consider two different boundary conditions. The first one is $g(x) = H(x)$. Since g is piecewise constant, the analysis given in sections 3-5 applies directly.

The second boundary condition is given by $g(x) = 0$ for $x < 0$, $g(x) = 2x$ for $0 \leq x \leq 1/2$ and $g(x) = 1$ for $x > 1/2$. Here, the boundary condition is not piecewise constant on each edge of the discretization, and the theory of sections 3-5 does not directly apply to the numerical solutions. However, the piecewise constant

h	1/25	1/50	1/100	1/200	1/400	1/800	$1/\infty$
L^1	1.5e-1	1.0e-1	6.7e-2	5.4e-2	3.9e-2	2.8e-2	0
order		0.50	0.45	0.49	0.47	0.48	0.5
L^2	1.7e-1	1.3e-1	1.1e-1	8.4e-2	6.6e-2	5.2e-2	0
order		0.37	0.32	0.33	0.34	0.33	0.33
L^∞	0.65	0.74	0.70	0.66	0.71	0.70	O(1)
order		-0.18	0.07	0.09	-0.10	0.03	0
step mt	1.4e-2	8.6e-3	5.5e-3	3.5e-3	2.2e-3	1.4e-3	0
order		0.74	0.64	0.66	0.69	0.66	0.67
linear mt	6.7e-4	2.6e-4	1.1e-4	4.2e-5	1.7e-5	6.6e-6	0
order		1.34	1.34	1.33	1.34	1.33	1.33
step 2d	1.1e-3	4.3e-4	1.8e-4	7.1e-5	2.8e-5	1.1e-5	0
order		1.36	1.39	1.32	1.34	1.31	1.33
linear 2d	7.1e-5	1.9e-5	5.0e-6	1.3e-6	3.3e-7	8.4e-8	0
order		1.90	1.93	1.95	1.97	1.98	2.0

Table 1. Errors for the step function boundary condition $g = 1$ for several values of h on the interval $(0, L = 2)$ for $\beta = \pi/3$.

approximation of piecewise linear functions is of order h in the L^2 norm; and regular moments of the approximation are of order h^2. Therefore, the numerical solution will display error estimates of the same order as those obtained in the theoretical sections.

We are interested in the convergence of $U_h(x, 1)$ to $U(x, 1)$ and $\bar{U}_h(x, y)$ to $U(x, y)$ for the different norms L^1, L^2, and L^∞. We also consider moments of the form

$$\int (U(x,1) - U_h(x,1))p(x)dx$$

for $p(x)$ piecewise constant and piecewise linear. To obtain a moment estimate that holds for all choices in a certain class of weight functions $p(x)$, we compute

$$\sup_z \left| \int (U(x,1) - U_h(x,1))p_z(x)dx \right|, \tag{53}$$

where $p_z(x) = w_{0z}(x) = 1 - H(z - x)$ for the piecewise constant moments, and $p_z(x) = w_{1z}(x) = 1$ for $x < z$, $p_z(x) = w_{1z}(x) =$

h	1/25	1/50	1/100	1/200	1/400	1/800	$1/\infty$
L^1	1.3e-2	4.6e-3	1.9e-3	7.4e-4	3.2e-4	1.3e-4	0
order		1.48	1.31	1.32	1.20	1.29	
L^2	1.5e-2	7.4e-3	3.2e-3	1.4e-3	7.7e-4	3.7e-4	0
order		1.03	1.21	1.16	0.89	1.06	1.00
L^∞	4.8e-2	2.8e-2	1.5e-2	6.9e-3	5.9e-3	3.4e-3	0
order		0.77	0.96	1.07	0.22	0.79	
step mt	1.3e-3	5.1e-4	2.1e-4	8.3e-5	3.2e-5	1.3e-5	0
order		1.40	1.28	1.34	1.35	1.31	1.33
linear mt	3.0e-3	5.6e-5	1.4e-5	3.6e-6	9.0e-7	2.3e-7	0
order		2.92	1.97	1.98	1.99	1.98	2.00
step 2d	4.3e-4	5.8e-4	1.4e-5	3.6e-6	9.0e-7	2.3e-7	0
order		2.90	2.00	2.00	2.00	2.00	2.00
linear 2d	1.2e-3	2.0e-4	4.9e-5	1.2e-5	3.1e-6	7.7e-7	0
order		2.59	2.00	2.00	2.00	2.00	2.00

Table 2. Errors for continuous, piecewise linear boundary condition g for several values of h on the interval $(0, L = 3)$ for $\beta = \pi/3$.

$z + 1 - x$ for $z \leq x \leq z + 1$ and $p_z(x) = w_{1z}(x) = 0$ for $x > z + 1$ for the continuous piecewise linear case.

The two dimensional moments we consider are of the form

$$\sup_z \Big| \int \int_{y_1}^{y_2} (U(x,y) - \bar{U}_h(x,y)) p_z(x) dy\, dx \Big|, \tag{54}$$

for the same weights p_z as above.

Our first computation is done with the step function boundary condition $g(x) = H(x)$. The solution was given for $N = 200$ in Fig. 3. The errors and orders of convergence are gathered in Table 1. The boundary condition $g(x)$ belongs to $H^s(\mathbb{R})$ for all $s < 1/2$. Therefore, we can apply Theorems 1 and 4 with $s < 1/2$, and consider to simplify the limit $s = 1/2$. This yields a rate of convergence of order $h^{1/3}$ for the L^2-norm. This is confirmed by the fifth row in Table 1. We deduce from section 4 that the L^∞ norm of the error does not converge to 0, and that the L^1 norm converges as $h^{1/2}$ (see rows 2-7 of Table 1).

The weights $w_{0z}(x)$ also belong to $H^t(0, L)$ for all $t < 1/2$ and all $z \leq L$. We do not need to consider coordinates $z > L$ since $(U - U_h)(x)$

is known to be exponentially small for $x \geq L$ (cf. section 4). We can apply Theorems 1 and 4 (with $u = v = 1$) with $s = 1/2$ and $t = 1/2$. Therefore, the step moment (53) with $p_z = w_{0z}$ converges as $h^{2/3}$ and the integrated (with $y_1 = 0$ and $y_2 = 1$) step moment (54) converges as $h^{4/3}$. This corresponds to the values of rows 9 and 13 in the table, respectively.

The weights $w_{1z}(x)$ belong to $H^s(0,L)$ for all $s < 3/2$. Therefore, we can replace $t = 1/2$ that held for the weights $w_{0z}(x)$ by $t = 3/2$ for this new weight. The error of convergence of (53) and (54) are therefore $h^{4/3}$ and h^2, respectively, as confirmed numerically in rows 11 and 15 of Table 1.

The second set of computations treats the continuous piecewise linear boundary condition $g(x) = 2x$ for $0 < x < 1/2$, and $g(x) = 1$ for $x \geq 1/2$. We have regrouped the numerical results in Table 2. The only difference with respect to the previous computation is the regularity of the boundary condition $g(x)$, which now belongs to every $H^s(0,L)$ for $s < 3/2$. Hence, we can apply Theorems 1 and 4 (still with $u = v = 1$) with $t = 3/2$. The accuracy of the L^2 norm and the different computed moments is therefore expected to be $h^{2/3}$ more accurate than for the step boundary condition, with a maximal accuracy of order h^2. This is confirmed by the numerical figures reported in Table 2.

Case with absorption. Let us now turn on the absorption constant γ. We consider the problem with step boundary condition $g(x) = H(x)$. We compute the L^2 norm of the error and the moment estimate (53) for $p_z = w_{1z}$. These two quantities are then divided by the L^2 norm of the exact solution, proportional to $e^{-\gamma/\nu}$. Hence, we can apply the results of Theorem 2 with $s = 1/2$ and $t = 3/2$. The numerical results are gathered in Table 3.

For small absorption, the convergence in the L^2 norm is expected to be of order $h^{1/3}$. This is verified for vanishing absorption (second row, fourth column of the Table). However, the results obtained for rather small absorption coefficients ($\gamma = 1$) already depart from this estimate (row 3, column 4). For larger absorption, $G(\gamma, h, 1/2, 0)$ is of order $h^{1/2}$. This is confirmed very satisfactorily by the results of column 4, rows 5-9. The convergence of the linear moment ($s = 1/2$ and $t = 3/2$) is of order $h^{4/3}$ for small absorption, as verified on column 8, row 2. For larger absorption, the estimate for $G(\gamma, h, 1/2, -3/2)$ for a fixed value of γ is of order h^2. We see that this estimate is better and better satisfied as γ grows (column 8, rows 3-9).

It remains to verify the validity of the coefficient $e^{\gamma/\nu}$ in the estimates. Let $\varepsilon(\gamma)$ be the error of DD for a given quantity (L^2 norm

γ	L^2 N=100	L^2 N=200	L^2 order	L^2 $\rho(\gamma)$	linear N=100	linear N=200	linear order	linear $\rho(\gamma)$
0	1.1e-1	8.4e-2	0.33		1.1e-4	4.2e-5	1.33	
1	1.3e-1	1.0e-1	0.39		1.3e-4	4.9e-5	1.44	
2	2.4e-1	1.8e-2	0.46	0.47	2.4e-4	7.6e-5	1.66	0.37
4	1.75	1.24	0.50	0.84	1.1e-3	2.7e-4	2.00	0.54
8	145	102	0.50	0.96	1.1e-1	2.6e-3	2.09	0.50
16	1.2e6	8.7e5	0.50	0.98	48	11	2.12	0.90
32	1.1e14	7.7e13	0.50	0.99	3.7e9	9.1e8	2.04	0.99

Table 3. Numerical simulations for different values of the absorption. The direction is $\beta = \pi/3$ and the interval is $(0, L = 3)$.

or linear moment here) and a given discretization mesh h. We define the quantity

$$\rho(\gamma) = \frac{\nu}{\gamma}\Big(\log[\varepsilon(2\gamma)] - \log[\varepsilon(\gamma)]\Big). \tag{55}$$

For an error of the form $\varepsilon(\gamma) = e^{\gamma/\nu} C_\varepsilon(h)$, where $C_\varepsilon(h)$ is a constant independent of γ, we see that $\rho(\gamma) \equiv 1$. So a value of ρ close to 1 corresponds to a good quality of the estimate $e^{\gamma/\nu} C_\varepsilon(h)$. The values of $\rho(\gamma)$ for the two problems (L^2 norm and linear moment), and for different values of N ($N = 100$ and $N = 200$) are given in columns 5 and 9 of the Table. As expected, this estimate is good when the error is larger than unity, that is to say when the Diamond Discretization does not capture the features of the exact solution at all. This threshold is $\gamma = 4$ for the L^2 norm for values of h of order 10^{-2}, and $\gamma = 16$ for the linear moment.

The above computation is typical of directions of propagation β that differ from $\pi/2$ and $\pi/4$. The case $\beta = \pi/2$ actually corresponds to a 1D problem since no information propagates laterally. We do not consider it here. The case $\beta = \pi/4$ is interesting in the sense that DD is exact when $\gamma = 0$. For positive absorption, the scheme produces some errors that do not behave as for other directions. The error estimates are given by Theorem 3. We see that the factor $e^{\gamma/\nu}$ is still present, but that the convergence as $h \to 0$ is of order h^{s+t} for moments of regularity H^t and boundary conditions of regularity H^s. We thus expect a faster convergence than for other directions, but still expect problems when γ becomes large. We present in Table 4 the same computations as above. Like for the other simulations, we found a very good agreement between the theory and the numerical computations.

γ	L^2 N=100	L^2 N=200	L^2 order	L^2 $\rho(\gamma)$	linear N=100	linear N=200	linear order	linear $\rho(\gamma)$
0	0	0	0.00		0	0	0.00	
1	9.3e-2	6.6e-2	0.50		1.0e-5	2.5e-5	2.00	
2	4.1e-1	2.9e-1	0.50	1.05	4.0e-4	1.0e-4	2.00	0.96
4	6.06	4.29	0.50	0.95	2.2e-3	5.5e-4	2.00	0.61
8	1.4e3	1.0e3	0.50	0.97	1.0e-1	2.7e-3	2.00	0.69
16	9.8e7	6.9e7	0.50	0.98	5.2e	1.3e	2.00	0.95
32	5.5e17	3.9e17	0.50	0.99	2.4e13	6.1e13	2.00	0.99

Table 4. Numerical simulations for different values of the absorption. The direction is $\beta = \pi/4$ and the interval is $(0, L = 3)$.

Notice to conclude that DD does not compute accurately the L^2 norm of the solution for moderate values of the absorption ($\gamma = 4$). However, higher moments of the solution, like linear moments, are still fairly well computed (relative error of 0.2% with $h = 10^{-2}$). Nevertheless, higher values of the absorption ($\gamma = 16$) become too high to be treated with DD, even if high moments of the solution are sought for.

Moments on small intervals. The weights $p_z(x)$ we have considered so far had a large support. It can be interesting in practice to have an estimate of the solution integrated over small regions. The theory given in sections 3-5 also applies to such cases. Consider for instance weights of the form

$$p_{\delta z}(x) = H(z) - H(z + h^\delta), \tag{56}$$

that is to say weights that equal 1 on $(z, z + h^\delta)$ and 0 elsewhere. The size of the interval depends on h. For sizes independent of h, even small, the asymptotic results as $h \to 0$ are the same as those shown above in this section.

We consider the case of a step boundary condition $g(x) = H(x)$. So we can apply Theorem 1 with $s = 1/2$. For piecewise constant functions, the H^s norm as $s \to 1/2$ essentially picks the jumps of the function. Since $p_{\delta z}$ has the same number of jumps independent

δ	N=50	N=100	order	N=200	order	N=400	order
0	8.7e-3	5.4e-3	0.69	3.5e-3	0.61	2.2e-3	0.69
1/3	3.5e-2	2.8e-2	0.33	2.0e-2	0.45	1.6e-2	0.35
2/3	1.6e-1	1.7e-1	-0.01	1.7e-1	0.00	1.7e-1	0.02

Table 5. Numerical computations of the moments (57) on small intervals of length h^δ for $\delta = 0$, $1/3$, and $2/3$. The direction is $\beta = \pi/3$ and the interval is $(0, L = 3)$.

of δ (and z), its H^t norm will be bounded for every $t < 1/2$, and of the same magnitude for every δ. We are interested in the error (53) normalized by the value expected for the moment. Since $U(x,1)$ is bounded and of order 1, we are thus interested in the normalized quantities

$$\sup_z \frac{\Big|\displaystyle\int (U(x,1) - U_h(x,1)) p_{z\delta}(x) dx\Big|}{\Big|\displaystyle\int p_{z\delta}(x) dx\Big|}. \tag{57}$$

Notice that here $\int p_{z\delta}(x)dx = h^\delta$. We deduce from Theorem 1 that such quantities are bounded by $Ch^{2/3(1/2+1/2)-\delta} = Ch^{2/3-\delta}$. We have gathered in Table 5 the results of (57) for values of δ equal to 0, 1/3, and 2/3. The computations have been performed for $h = 1/N$, with $N = 50$, $N = 100$, $N = 200$, and $N = 400$. The order of convergence of the method theoretically equals 0.67 for $\delta = 0$, 0.33 for $\delta = 1/3$, and 0 for $\delta = 2/3$. This is confirmed by columns 4, 6, and 8 of the table.

8. Conclusions

We have used a quite established method, the Fourier analysis of linear scalar hyperbolic equations, to obtain a global understanding of the spurious modes generated by a very popular spatial discretization used in particle transport theory, the Diamond Discretization. We have obtained theoretical estimates of the error between the discretized and the continuous solutions for different norms as well as estimates of the moments of the error. Even though DD may be converging slowly to the exact solution in the L^2 norm for non smooth boundary conditions, suitable moments of the discrete solutions still display an accuracy of order h^2, as noticed numerically in [16]. We have shed some new light on the role of absorption and the total inadequacy of DD to correctly attenuate high frequency modes. These results delimit the domain of accuracy of DD depending on the information sought for (L^2 norms or spatial moments). In any case, they confirm the validity of DD for computing particle distributions in diffusive media, where absorption is weak and propagation along straight lines short, and show that DD should be used with care when dealing with the propagation of particles for long distances as shown in [18].

Acknowledgment

The author would like to thank Ed Larsen for his many helpful comments and suggestions during the preparation of this work. This work was supported in part by NSF grant DMS-0072008, in part by the ASCI Flash Center at the University of Chicago under DOE contract B341495 and in part by the MRSEC Program of the National Science Foundation under Award Number DMR-9808595.

References

1. R. A. Adams, *Sobolev Spaces*, Academic Press, NY, San Francisco, London, 1975.
2. M. Apelkrans, *On Difference Schemes for Hyperbolic Equations with Discontinuous Initial Values*, Math. Comp., 22 (1968), pp. 525–539.
3. S. R. Arridge, *Optical tomography in medical imaging*, Inverse Problems, 15 (1999), pp. R41–R93.
4. S. R. Arridge, H. Dehghani, M. Schweiger, and E. Okada, *The finite element model for the propagation of light in scattering media: A direct method for domains with nonscattering regions*, Med. Phys., 27(1) (2000), pp. 252–264.
5. G. Bal and M. Moscoso, *Polarization Effects of Seismic Waves on the Basis of Radiative Transport Theory*, Geophys. J. Int., 142(2) (2000), pp. 571–585.
6. K. M. Case and P. F. Zweifel, *Linear Transport Theory*, Addison-Wesley series in nuclear engineering, Addison-Wesley, Reading, Mass., 1967.
7. S. Chandrasekhar, *Radiative Transfer*, Dover Publications, New York, 1960.
8. P. G. Ciarlet and J.-L. Lions, eds., *Handbook of numerical analysis*, North-Holland, Amsterdam, 1990.
9. J. J. Duderstadt and W. R. Martin, *Transport Theory*, Wiley-Interscience, New York, 1979.
10. R. C. Gunning and H. Rossi, *Analytic Functions of Several Complex Variables*, Prentice Hall, INC., Englewood Cliffs, N.J., 1965.
11. G. W. Hedstrom, *The rate of convergence of some difference schemes*, SIAM J. Num. Anal., 5(2) (1968), pp. 363–406.
12. ———, *Models of difference schemes for $u_t + u_x = 0$ by partial differential equations*, Math. Comp., 29 (1975), pp. 969–977.

13. A. H. Hielscher, R. E. Alcouffe, and R. L. Barbour, *Comparison of finite-difference transport and diffusion calculations for photon migration in homogeneous and heterogeneous tissues*, Phys. Med. Biol., 43 (1998), pp. 1285–1302.
14. A. Ishimaru, *Wave Propagation and Scattering in Random Media*, New York: Academics, 1978.
15. C. Johnson and J. Pitkäranta, *An analysis of the discontinuous Galerkin method for a scalar hyperbolic equation*, Math. Comp., 46(173) (1986), pp. 1–26.
16. E. W. Larsen, *Spatial Convergence Properties of the Diamond Difference Method in X,Y-Geometry*, Nuclear Science and Engineering, 80 (1982), p. 710.
17. E. E. Lewis and W. F. Miller Jr., *Computational Methods of Neutron Transport*, J. Wiley and sons, New York, 1984.
18. K. A. Mathews, *On the Propagation of Rays in Discrete Ordinates*, Nucl. Sci. Eng., 132 (1999), pp. 155–180.
19. R. D. Richtmyer and K. W. Morton, *Difference Methods for Initial Value Problems*, 2nd ed., Interscience, New York, 1967.
20. L. Ryzhik, G. Papanicolaou, and J. B. Keller, *Transport equations for elastic and other waves in random media*, Wave Motion, 24 (1996), pp. 327–370.
21. H. Sato and M. C. Fehler, *Seismic wave propagation and scattering in the heterogeneous earth*, AIP series in modern acoustics and signal processing, AIP Press, Springer, New York, 1998.
22. V. Thomée, *Stability theory for partial difference operators*, SIAM Rev., 11(2) (1969), pp. 152–195.
23. G. B. Whitham, *Linear and Nonlinear waves*, Wiley Interscience, New York, 1974.